SUPPORTING INFROMATION

A New All-Aqueous Thermally Regenerative Ammonia Battery Using the Cu(I, II) Redox Reaction

Renaldo Springer[1,2], Nicholas Cross[3], Serguei N. Lvov[1,2,4,] Bruce E. Logan[5], Christopher A. Gorski[5], Derek M. Hall[1,2,z]

[1]The EMS Energy Institute, The Pennsylvania State University, University Park, PA, USA
[2]Department of Energy and Mineral Engineering, The Pennsylvania State University, University Park, PA, USA
[3]Department of Chemical Engineering, The Pennsylvania State University, University Park, PA, USA
[4]Department of Materials Science and Engineering, The Pennsylvania State University, University Park, PA, USA
[5]Department of Civil and Environmental Engineering, The Pennsylvania State University, University Park, PA, USA
[z]Corresponding Author. hall@psu.edu, 166 Energy and Environment Laboratory, The Pennsylvania State University, University Park, PA 16802, USA.

Thermodynamic Calculations

This section outlines the various thermodynamic values and calculations used to determine ligand complexation potential for the catholyte and the anolyte. **Table S1** contains the Cu(I, II)-ligand redox reactions used to analyze speciation. Speciation calculations were conducted through the formulation of mass balance and equilibrium constant equations, an example of which is shown for the Cu(I, II)-Cl complexation reaction in **Calculation S1**. The speciation values are approximate as we assumed the activity coefficients for each species are 1. Our previous studies included activity coefficients in the potential calculations, and the resulting potentials changed by a few percent but it did not change the trends observed substantially. [17,27] **Tables S2, S3 and S4** is a compilation of equilibrium potential values found in literature and used in calculation S1**.**

Table S1. Metal-ligand complexation reactions for Cu(I, II) aqueous species.

	Chloride	**Bromide**	**Ammonia**
Cu(I)	$Cu^+ + Cl^- = CuCl^0$ $CuCl^0 + Cl^- = CuCl_2^-$ $CuCl_2^- + Cl^- = CuCl_3^{2-}$	$Cu^+ + Br^- = CuBr^0$ $CuBr^0 + Br^- = Cu(Br)_2^-$ $Cu(Br)_2^- + Br^- = Cu(Br)_3^{2-}$	$Cu^+ + NH_3 = Cu(NH_3)^+$ $Cu(NH_3)^+ + NH_3 = Cu(NH_3)_2^+$ $Cu(NH_3)_2^+ + NH_3 = Cu(NH_3)_3^+$
Cu(II)	$Cu^{2+} + Cl^- = CuCl^+$ $CuCl^+ + Cl^- = CuCl_2$ $CuCl_2 + Cl^- = CuCl_3^-$ $CuCl_3^- + Cl^- = CuCl_4^{2-}$	$Cu^{2+} + Br^- = CuBr^+$ $CuBr^+ + Br^- = Cu(Br)_2$ $Cu(Br)_2 + Br^- = CuBr_3^-$ $CuBr_3^- + Br^- = CuBr_4^{2-}$	$Cu^{2+} + NH_3 = Cu(NH_3)^{2+}$ $Cu(NH_3)^{2+} + NH_3 = Cu(NH_3)_2^{2+}$ $Cu(NH_3)_2^{2+} + NH_3 = Cu(NH_3)_3^{2+}$ $Cu(NH_3)_3^{2+} + NH_3 = Cu(NH_3)_4^{2+}$ $Cu(NH_3)_4^{2+} + NH_3 = Cu(NH_3)_5^{2+}$

Calculation S1. System of equations used to determine the ligand speciation concentrations. In these calculations we assumed the activity coefficients ($\gamma_{\pm}$) were equal to one.

$$K_1 = \frac{\gamma_{\pm} b_{CuCl+}}{\gamma_{\pm} b_{Cu2+}\ \gamma_{\pm}\ b_{Cl-}} \quad [S.1]$$

$$K_2 = \frac{\gamma_{\pm} b_{CuCl2}}{\gamma_{\pm} b_{CuCl+}\ \gamma_{\pm} b_{Cl-}} \quad [S.2]$$

$$K_3 = \frac{\gamma_{\pm} b_{CuCl3-}}{\gamma_{\pm} b_{CuCl2}\ \gamma_{\pm} b_{Cl-}} \quad [S.3]$$

$$K_4 = \frac{\gamma_{\pm} b_{CuCl42-}}{\gamma_{\pm} b_{CuCl3-}\ \gamma_{\pm}\ b_{Cl-}} \quad [S.4]$$

Mass Balance Equations:

Total $b_{Cl-} = b_{Cl-} + b_{CuCl+} + 2b_{CuCl2} + 3b_{CuCl3-} + 4b_{CuCl42-}$ [S.5]

Total $b_{Cu2+} = b_{Cu2+} + b_{CuCl+} + b_{CuCl2} + b_{CuCl3-} + b_{CuCl42-}$ [S.6]

Table S2. The equilibrium constants for the Cu(I)-ligand aqueous complexes.

K_{eq}	**Chloride**[17]	**Bromide**[44]	**Ammonia**[24]
1	1.34E+04	3.39E+03	5.50E+05
2	2.06E+01	2.14E+02	9.12E+04
3	2.03E-01	3.72E+00	6.30E-01
4	-	-	-

Table S3. The equilibrium constants for the Cu(II)-ligand aqueous complexes.

K_{eq}	**Chloride**[17]	**Bromide**[45]	**Bromide**[46]	**Ammonia**[25]	**Ammonia**[29]
1	2.51E+00	1.42E+01	4.79E+05	7.25E+05	1.20E+04
2	8.13E-02	3.97E-02	3.63E+01	8.17E+06	3.00E+03
3	2.51E-02	-	4.79E+00	3.75E+04	8.00E+02
4	5.01E-03	-	3.70E-01	6.06E+03	1.20E+02
5	-	-	-	1.19E+01	3.00E-01

Table S4. The equilibrium potential, E_{eq}, for the Cu(II)-NH_3 aqueous complexes through speciation analysis, referencing different thermodynamic sources.

Concentration	**Ammonia**[25]	**Ammonia**[29]
1 mol kg^{-1}	-0.513 V	0.053 V
4 mol kg^{-1}	-0.602 V	-0.016 V

EIS Analysis of RDE data

This section highlights the steps used to gather kinetic information for the Cu(I, II) complexation reactions from the RDE system. **Figure S1** is the Randles equivalent circuit used to analyze the RDE EIS data. **Figure S2** highlights the accuracy of the fitted equivalence circuit data to the raw data. **Figure S3** shows the influence of increased rotation rate on the electrode kinetics. **Table S5** shows an example of the data retrieved from the EIS fit. **Table S6** shows the exchange current density values and the impact of ligand concentrations, calculated using EIS fit data.

The Randles cell equivalent circuit, which accounts for the ohmic resistance of the electrolyte solution, R_s, finite length Warburg impedance, W_{s1}, constant phase element, CPE ($CPE_{1\text{-}T}$ and $CPE_{1\text{-}P}$)[19] and the charge transfer resistance, R_{ct}[47], was used to quantify how ligands influence the charge transfer process (**Figure S1**).

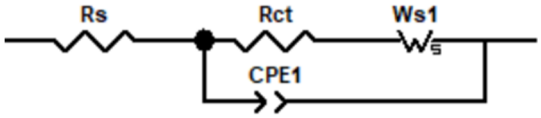

Figure S1. Randles Equivalent Circuit Model

Using EIS and the Randle cell circuit model, charge transfer resistance (R_{ct}) were used to calculate j_0 values [30] of the Cu(I, II) redox reaction for Pt and GC electrode surfaces. **Equation S.7** relates R_{ct} to j_0, where A is the geometric electrode area.

$$j_0 = RT\,(FAR_{ct})^{-1} \quad \text{[S.7]}$$

Ligand effects on R_{ct} were converted to exchange current density (j_0) values, which are proportional to R_{ct} values obtainable through a Randle cell model. Equivalent circuit predictions (**Figure S2**) closely matched the experimental data supporting the use of a Randle circuit model. Changes in the R_{ct} value (**Table S5**) showed the impact of the surface material on the high-frequency semi-circle, indicating the reaction is faster on Pt relative to GC surfaces.

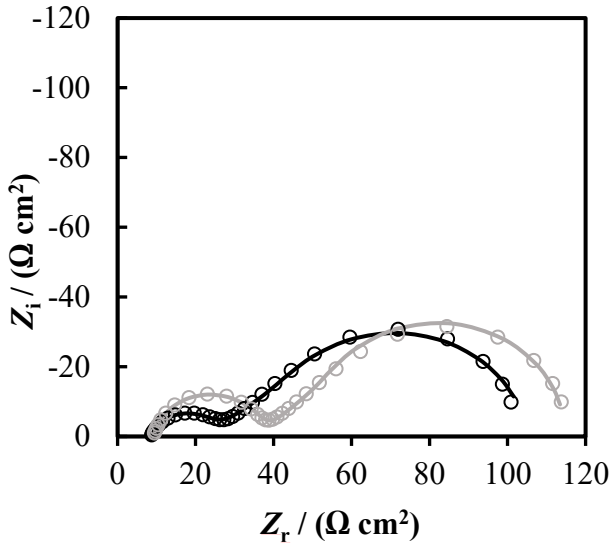

Figure S2. EIS data (circles) and fitting (lines) of RDE data for GC (grey) and Pt (black) working electrodes. Conditions: 500 RPM, 1 mol/kg NH_4Cl(aq), 25 ºC and 1 bar.

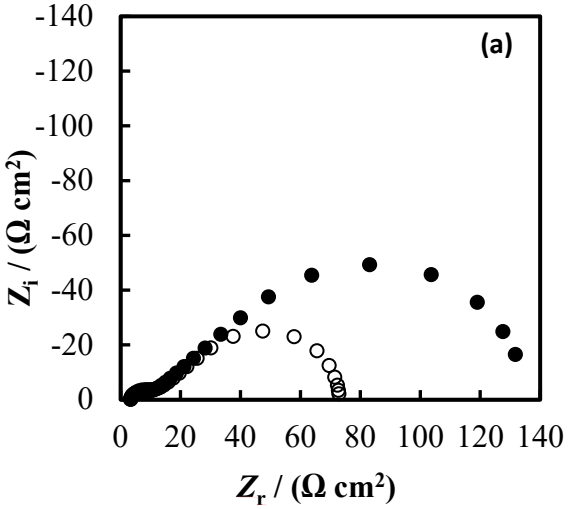

Figure S3. (a) Nyquist plots collected from an RDE using the Pt working electrode at 500 RPM (•) and 2000 RPM (○). Conditions: 4 mol kg^{-1} NH_4Cl(aq), 25 ºC and 1 bar.

The Randles cell equivalent circuit produces values based on the curve fit as shown in Table S5, where $R_{ohm,}$ is the solution resistance. W_R , W_P and W_T are parameters for the Warburg element. The R_{ct} values were used to obtain the exchange current densities presented in S6.

Table S5. Circuit model values used to fit the EIS spectra shown in **Figure 5**.

Circuit Element	GC Surface	Pt Surface
R_{ohm} / Ω	9.36 ± 0.04	8.59 ± 0.05
R_{ct} / Ω	27.56 ± 0.12	17.76 ± 0.16
W_R / Ω	77.84 ±0.44	75.64 ± 0.48
W_T	0.57 ± 0.01	0.57 ± 0.01
W_P (fixed)	0.5	0.5
$CPE_{1\text{-}T}$ / F	6.15E-06 ± 0.27E-6	4.10E-05 ± 0.29E-5
$CPE_{1\text{-}P}$	0.89 ± 0.01	0.78 ± 0.01

The j_0 values obtained were large (**Table S6**) indicating that the Cu(I,II) redox reaction is fast, with j_0 values larger than the hydrogen evolution reaction on Pt.[48]

Table S6. j_0 values for the Cu(I, II) redox reaction with Pt and GC working electrodes at 25 ºC and 1 bar.

Ligand	b_L / mol kg^{-1}	$j_{0(Pt)}$ / mA cm^{-2}	$j_{0(GC)}$ / mA cm^{-2}
NH_3(aq)	1	8 ± 1	7.1 ± 0.2
	4	10 ± 1	8.4 ± 0.1
Cl^-(aq)	1	15 ± 4	5 ± 0.5
	4	35 ± 11	8.4 ± 0.1
Br^-(aq)	1	28 ± 5	6 ± 2.0
	4	79 ± 23	29 ± 10

LSV Analysis of RDE data

This section analyzes linear sweep voltammetry results to gain information regarding transfer coefficients. **Figure S4** shows LSV plots for each ligand, highlighting potential shifts and limiting current values. **Figure S5** is an example of the Newton-Raphson fit done on the LSV data to estimate the transfer coefficients. **Table S7** shows the changes in transfer coefficients based on electrode material of both the ligand and concentration.

The generalized Butler-Volmer (B-V) equation was used to determine the transfer coefficients (α_c) via the nonlinear fitting of LSV data using the Newton-Raphson method.[19,32]

$$j = \frac{\exp[(1-\alpha_c)(\frac{F\eta}{RT})]-\exp[(-\alpha_c)(\frac{F\eta}{RT})]}{(\frac{1}{j_0})+(\frac{1}{j_{lim,a}})\ \exp[(1-\alpha_c)\left(\frac{F\eta}{RT}\right)]-(\frac{1}{j_{lim,c}})\ \exp[(-\alpha_c)\left(\frac{F\eta}{RT}\right)]} \quad \text{[S.8]}$$

where j is the current density, $j_{lim,a}$ is the anodic limiting current density, $j_{lim,c}$ is the cathodic limiting current density and η is the overpotential, F is Faraday's Constant, R is the gas constant, T is the thermodynamic temperature, and α_c is the transfer coefficient.

Values for $j_{lim,a}$ and $j_{lim,c}$ were obtained directly from the LSV plots, while j_0 values were obtained from EIS tests. Rate constants (k_0) of the Cu(I, II) redox reactions were calculated using **Equation 9**[17], where c_{ox} and c_{red} are concentrations (mol cm^{-3}) of the oxidation and reduction species, respectively:

$$j_0 = Fk_0(c_{ox}^{1-\alpha_c} c_{red}^{\alpha_c}) \quad \text{[S.9]}$$

The transfer coefficient (α_c) in **Equation S.8** is the same used in **Equation S.9**.

The polarization curves obtained through LSV analysis, indicated the limiting currents had minimal variation between ligands, relative to changes in j_0 and by relation k_0. The RDE potential of the working electrode is E_w (i.e. corrected for the solution resistance and reference electrode potential) (**Figure S4**). The limiting current densities obtained from LSV data agreed with trends observed with EIS data showing that the diffusion layer thickness impacted limiting currents far more than differences between diffusion coefficients of the different complexes.

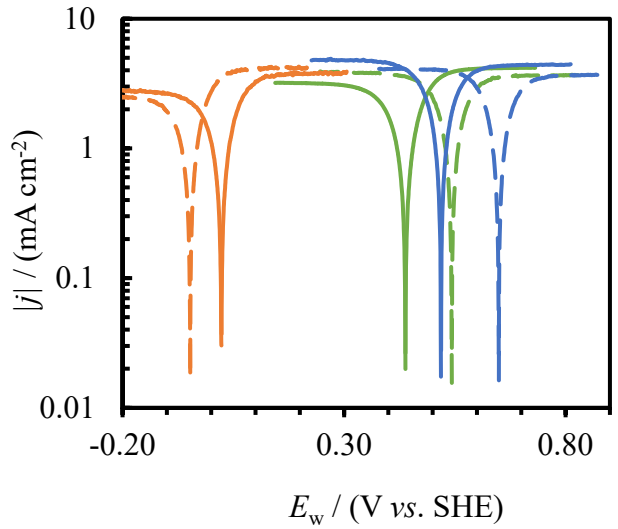

Figure S4. RDE LSV data highlighting the impacts of complexation on the Cu(I, II) redox reaction with 4 mol kg^{-1} (dashed lines) and 1 mol kg^{-1} (solid lines) solutions of NH_3(aq) (orange), NH_4Br(aq) (blue) and NH_4Cl(aq) (green). Conditions: 25 °C and 1 bar at 500 RPM.

Another observation was the small charge-transfer controlled regions of the Cu(I, II) reactions, indicating favorable kinetics, as little overpotential was required to reach the limiting current. Tafel analysis would ideally indicate symmetric polarization curves for both anodic and cathodic regions.[19] However, the small charge-transfer region, indicative of facile kinetics, made Tafel and Koutecky-Levich analysis difficult. This is shown through non-linear fitting, which indicated that transfer coefficients, α_c, still impacted the polarization curves. The influence of α_c can be clearly seen if values of α_c are varied from 0.3 to 0.8 as the resulting curves clearly deviate from the experimentally obtained data in both cathodic and anodic regions (**Figure S5**).

Overall, ligand concentration, ligand type and surface materials only slightly changed α_c. Increasing the ligand concentration, consistently decreased the transfer coefficients, and for the most part, the coefficients were larger with GC *vs*. Pt. Unlike j_0 and E_{eq} values, no obvious trends were observed between the coefficients and ligand field strength (**Table S7**).

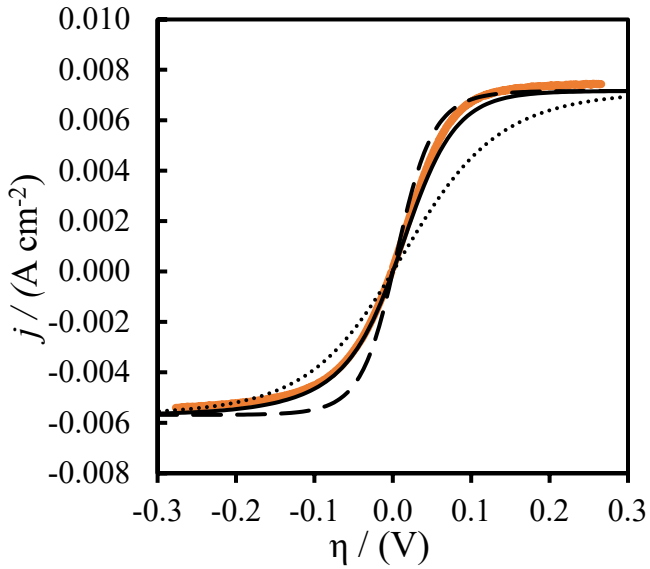

Figure S5. LSV data of Cu (I, II)-NH_3 complex data (orange) with a GC working electrode at 1 mol kg^{-1} NH_3(aq) and non-linear fitting results with Equation 6 indicating $\alpha_c = 0.38$ (solid black) and polarization curves from Equation 6 assuming $\alpha_c = 0.3$ (dashed) and 0.8 (dotted). Conditions: 2000 RPM, at 25 ºC and 1 bar.

Table S7. Ligand complexation impact on the charge transfer coefficients of the Cu(I, II) redox reaction for Pt and GC working electrodes at 25 ºC and 1 bar.

Ligand	b_L **/ mol** kg^{-1}	$\alpha_{c,Pt}$ (± 1 %)	$\alpha_{c,GC}$ (± 1 %)
NH_3(aq)	1	0.34	0.38
	4	0.28	0.25
Cl^-(aq)	1	0.35	0.50
	4	0.30	0.48
Br^-(aq)	1	0.37	0.42
	4	0.30	0.33

Full Cell Charge/Discharge Curves

The charge discharge curves for the Br-NH_3 all-Aq TRAB indicated a good first cycle with steep decreases in successive cycles (**Figure S6**). Although this would not matter in a TRAB, since the electrolytes would be regenerated after the 1st cycle, it still indicates the possibility of this chemistry to be used in other electrochemical systems.

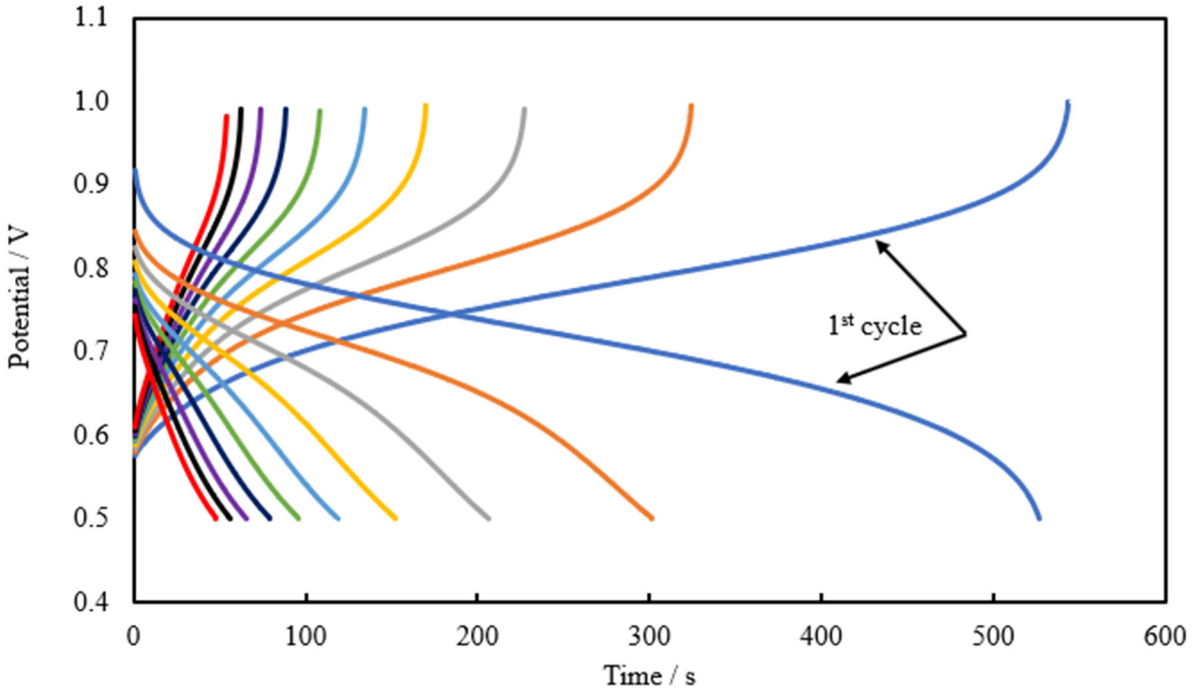

Figure S6. Charge and discharge curves for the Br-NH_3 all-Aq TRAB after 10 cycles at 25 ^{o}C and 1 bar with 0.5 mol kg-1 of total Cu.